

SNR 0104-72.3: A REMNANT OF TYPE IA SUPERNOVA IN A STAR-FORMING REGION?

JAE-JOON LEE^{1,2} SANGWOOK PARK³, JOHN P. HUGHES⁴, PATRICK O. SLANE⁵, AND DAVID N. BURROWS⁶

Draft version November 2, 2018

ABSTRACT

We report our 110 ks *Chandra* observations of the supernova remnant (SNR) 0104-72.3 in the Small Magellanic Cloud (SMC). The X-ray morphology shows two prominent lobes along the northwest-southeast direction and a soft faint arc in the east. Previous low resolution X-ray images attributed the unresolved emission from the southeastern lobe to a Be/X-ray star. Our high resolution *Chandra* data clearly shows that this emission is diffuse, shock-heated plasma, with negligible X-ray emission from the Be star. The eastern arc is positionally coincident with a filament seen in optical and infrared observations. Its X-ray spectrum is well fit by plasma of normal SMC abundances, suggesting that it is from shocked ambient gas. The X-ray spectra of the lobes show overabundant Fe, which is interpreted as emission from the reverse-shocked Fe-rich ejecta. The overall spectral characteristics of the lobes and the arc are similar to those of Type Ia SNRs, and we propose that SNR 0104-72.3 is the first case for a robust candidate Type Ia SNR in the SMC. On the other hand, the remnant appears to be interacting with dense clouds toward the east and to be associated with a nearby star-forming region. These features are unusual for a standard Type Ia SNR. Our results suggest an intriguing possibility that the progenitor of SNR 0104-72.3 might have been a white dwarf of a relatively young population.

Subject headings: ISM: individual objects (SNR 0104-72.3) — ISM: supernova remnants — X-rays: ISM

1. INTRODUCTION

Among about a dozen supernova remnants (SNRs) detected in the Small Magellanic Cloud (SMC), only three X-ray brightest SNRs (0102-72.3, 0103-72.6, and 0049-73.6) have been relatively well studied. Because all these three SNRs most likely originate from a core-collapse SN, revealing the type of other SNRs is of great importance to study the star-forming history, SN rates, and chemical evolution of the SMC. SNR 0104-72.3 is the fourth brightest X-ray SNR in the SMC, whose origin has been controversial. Its optical emission was suggested to be Balmer-dominated (Mathewson et al. 1984), indicating Type Ia origin. On the other hand, with the ROSAT data, Hughes & Smith (1994) identified an unresolved X-ray source in the southern part of the SNR as a candidate Be/X-ray star which appeared to be co-spatial with the SNR. Based on this plus other evidence for a Population I environment, they suggested a core-collapse origin for SNR 0104-72.3. With the XMM-Newton data, van der Heyden et al. (2004) found evidence for enhanced Fe L line emission from the remnant, with which they reinstated Type Ia origin. Recently, with Akari IRC observations, Koo et al. (2007) discovered bright infrared shells which are positionally coincident with the optical H α filaments surrounding the X-ray emission (Hughes & Smith 1994). IR color distribu-

tions indicated shock interaction with ambient molecular clouds, which may support a core-collapse explosion of a massive progenitor star for the origin of SNR 0104-72.3.

We report here on the results from our observations of SNR 0104-72.3 with the *Chandra* X-Ray observatory. We note that the remnant has been serendipitously detected a number of times by *Chandra* during the ACIS calibration observations of SNR 0102-7219. However, SNR 0104-72.3 was detected mostly in FI CCDs at large off-axis angles. Due to the low sensitivity and the poor spatial resolution, these archival data were not suitable for our analysis and we only report results based on our new observations.

2. OBSERVATION & RESULTS

We observed SNR 0104-72.3 with the Advanced CCD Imaging Spectrometer (ACIS) on board *Chandra* on 2008 Jan 27–31 during AO9. We used ACIS-S3 for the effective detection of the soft X-ray emission of the SNR. A total of 110 ks of exposure, with two separate obsIDs (54 ks for obsID 9100, 56 ks for obsID 9810) was obtained in the VFaint mode. The level 1 event files were reprocessed to create new level 2 event files. We applied parameters of the standard *Chandra* pipeline process, except that we applied the VFaint mode background cleaning and turned off the pixel randomization. CIAO 4.2 and CALDB 4.2.2 were used for all the reprocessing and analysis. We examined the overall background light curve for periods of high background. No significant background flare was seen and we did not apply any light curve filtering.

3. X-RAY IMAGES

Figure 1(a) is the broad band (0.6-3.0 keV) *Chandra* ACIS image of SNR 0104-72.3. Our deep ACIS image reveals details of the X-ray structures that have not been available from the previous ROSAT

¹ Korea Astronomy and Space Science Institute, Daejeon 305-348, Korea

² leejjoon@kasi.re.kr

³ Department of Physics, University of Texas at Arlington Arlington, TX 76019

⁴ Department of Physics and Astronomy, Rutgers University, 136 Frelinghuysen Road, Piscataway, NJ 08854-8019

⁵ Harvard-Smithsonian Center for Astrophysics, 60 Garden Street, Cambridge, MA 02138

⁶ Astronomy and Astrophysics Department, Pennsylvania State University, University Park, PA 16802

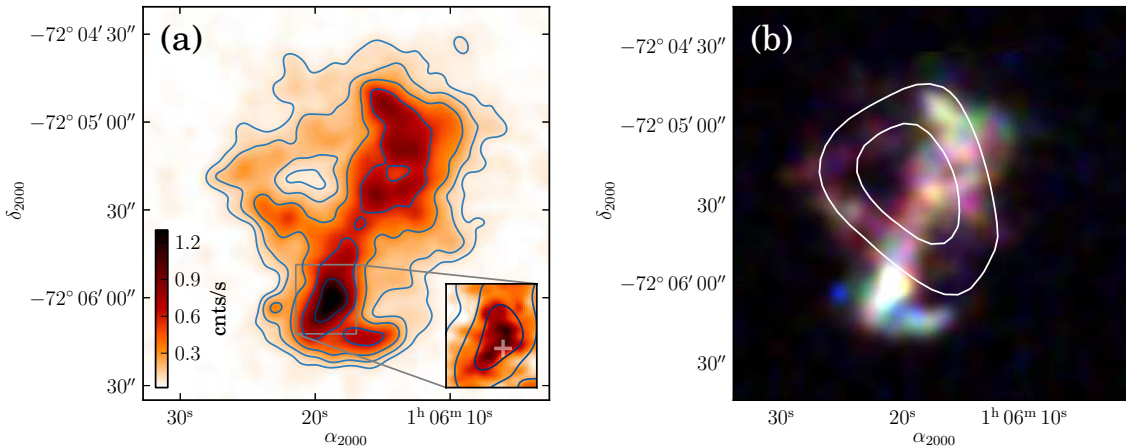


FIG. 1.— (a) Chandra image (0.6-3.0 keV) of SNR 0104-72.3 smoothed with Gaussian beam of $2.5''$. (inset) zoom-up of the bright southern lobe, where previous observations suggested as a point source, smoothed with $1''$ beam. The location of the candidate Be star is marked with a white plus sign. (b) RGB composite image of the Chandra data overlaid with white contours of the 843 MHz radio map (Bock et al. 1999). Red is 0.6-0.95 keV, green is 0.95-1.12 keV, and blue is 1.12-3 keV bands.

and XMM-Newton observations (Hughes & Smith 1994; van der Heyden et al. 2004). The X-ray morphology of the remnant is dominated by bright lobes extending about $90''$ along the northwest-southeast direction. Faint emission surrounding the lobes is also clearly seen. Most notably, there is a faint arc-like structure on the eastern side of the lobes. We refer to the region including two lobes as the “bar” region, and the faint arc emission in the east as the “arc” region (see inset image of Figure 2(a)). Figure 1(b) shows a RGB composite image of SNR 0104-72.3. The bar and the arc regions show different colors in the RGB image. The arc is dominated by red while the bar shows a complex mixture of three colors. A color variation is also noticed within the bar, where the bright southern and northern regions of the bar are more greenish (i.e., 0.95-1.12 keV) and/or blueish (i.e., 1.12-3 keV) than the regions in the middle. There is thus a trend of higher photon energies toward the ends of the bar than in the middle.

4. SPECTRAL ANALYSIS

The high-resolution ACIS imaging observations allow us to perform a spatially resolved spectral analysis of SNR 0104-72.3. We extracted X-ray spectra from several characteristic regions, based on the color variation in the RGB composite image. For a background subtraction, we used an average spectrum from four circular regions ($\sim 30''$ in radius) around the SNR. For spectral modeling, unbinned spectra were fit using the Churazov weighting (Churazov et al. 1996).

We first extract spectra from the arc and the bar. The background-subtracted spectra are shown in Figure 2. The observed spectra are soft, with most of the emission seen below 3 keV. The peak energy of the arc is lower than that of the bar, which explains the different color between the arc and the bar in Figure 1(b). We fit the spectra with a single nonequilibrium ionization (NEI) plane-parallel shock model (Borkowski et al. 2001, vpshock in Xspec v12) that is based on ATOMDB (Smith et al. 2001). We use an augmented version of this atomic database to include inner-shell processes and

updates of the Fe L-shell lines.⁷ We modeled the foreground absorption by the Galaxy and the SMC separately. For the absorption by the Galaxy, we used a fixed column density of $N_{\text{H,Gal}} = 2.2 \times 10^{20} \text{ cm}^{-2}$ which is the H I column density of the Galaxy toward SNR 0104-72.3 (Dickey & Lockman 1990). The foreground column density in the SMC ($N_{\text{H,SMC}}$) is fit as an additional absorption component assuming the SMC interstellar abundances (Russell & Dopita 1992). We first try to fit the spectra with elemental abundances of the emitting gas fixed at those of the SMC values (Russell & Dopita 1992). An acceptable fit is obtained for the spectrum of the arc region. The best fit results give hydrogen column density of $N_{\text{H,SMC}} \sim 1 \times 10^{22} \text{ cm}^{-2}$ and an electron temperature of 0.54 keV, although the ionization time scale is poorly constrained. This is the region where the remnant is thought to interact with dense ambient gas (see § 5), and the X-ray spectral fit result is consistent with such an interpretation, i.e., the X-ray emission of the arc is predominantly from shocked gas with SMC abundances. On the other hand, the spectrum of the bar region cannot be adequately fit with models using SMC abundances (reduced chi-squared ~ 3); the prominent peak near 1 keV, in particular, could not be reproduced. The strong lines in this energy range are those of Ne K and Fe L shell lines. Freeing abundances of Ne and Fe provides an acceptable fit. The best fit model has overabundant Fe (by a factor of 10 increase above the SMC value) and negligible amount of Ne. We note that quantitative interpretations of the Fe abundance are difficult due to several modeling issues including incomplete Fe L line modeling (e.g., Badenes et al. 2006), and we interpret this number only in general sense of the Fe-rich ejecta. Our results of the Fe overabundance is consistent with the results of van der Heyden et al. (2004). The H I column density of the SMC toward SNR 0104-72.3 is $\sim 6 \times 10^{21} \text{ cm}^{-2}$ (Stanimirovic et al. 1999). While the estimated $N_{\text{H,SMC}} \sim 9 \times 10^{21} \text{ cm}^{-2}$ is slightly larger than the H I column density, we note that HI column

⁷ The augmented APEC atomic data have been provided by K. Borkowski. The relevant discussion on these detailed plasma model issues has been presented in Badenes et al. (2006).

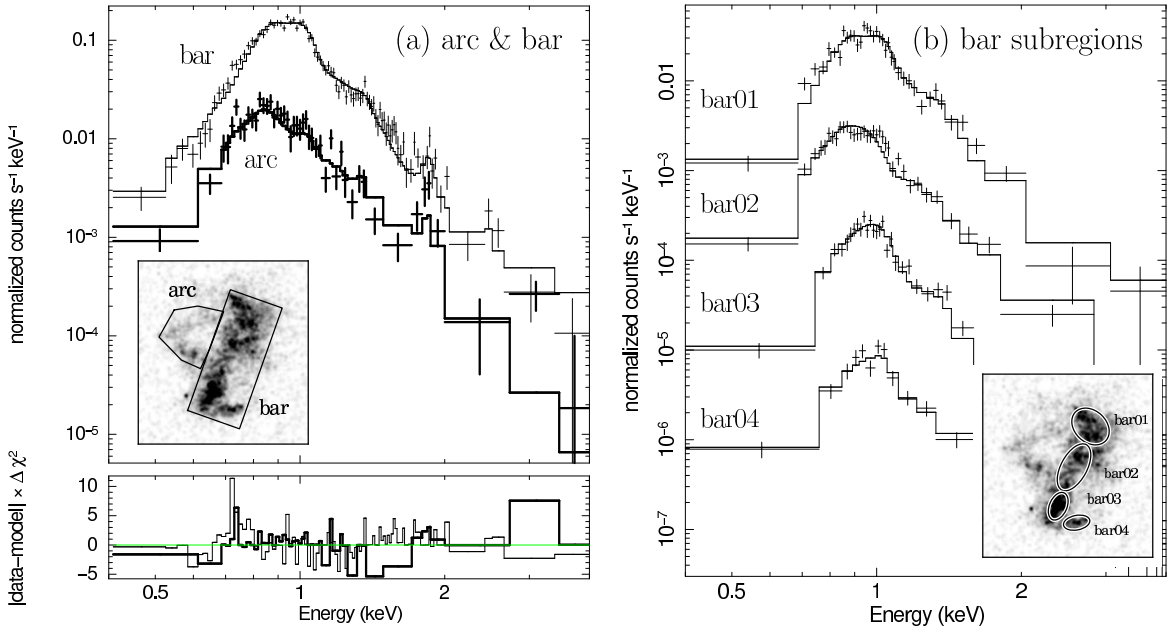


FIG. 2.— (a) Chandra spectra of the bar and the arc regions. The inset image shows the extraction regions of the spectra. The solid lines are best fit models in Table 1. The spectra are binned for display purpose only. (b) Chandra spectra of subregions of the bar. The inset image shows the extraction regions of the spectra. The spectra of bar02, bar03, bar04 are scaled by 10^{-1} , 10^{-2} and 10^{-3} , respectively for a display purpose. The solid lines are best fit models in Table 1, scaled accordingly.

density values typically underestimate the total hydrogen column density.

The RGB composite image in Fig. 1(b) shows varying colors within the bar region, indicating spectral variations although some of them may be simply due to low photon statistics. Figure 2(b) shows extracted spectra from 4 smaller regions inside the bar, and spectra of some regions (e.g., bar04) show slightly different spectra than others. We fit spectra from each subregion with the vps shock model. Because of the poor photon statistics of individual regions, we could not constrain model parameters with both Ne and Fe abundances varied in the fits. Thus, as the previous fit results of the bar suggested negligible contribution of Ne, we fix Ne at the SMC abundance (fixing it at the best fit parameter of the bar region has only minor effect on the results). We further fix the absorbing column density at the best fit parameter of the bar region ($N_{\text{H,SMC}} = 9.1 \times 10^{21} \text{cm}^{-2}$). This approach provides an acceptable fit with reasonable parameter constraints. We find that the spectra from the central regions tend to have lower temperature and lower Fe abundance. The origin of this spectral variation is unclear with the current data. We speculate that the thermal conditions and/or metal abundances may be inhomogeneous along the bar region, possibly due to the mixture of the ejecta and ambient medium and/or intrinsically non-uniform distribution of the ejecta. And the spectral fits suggest that the central regions may be less dominated by ejecta material. All the fit results are tabulated in Table 1.

5. DISCUSSION

5.1. The SN type of SNR 0104-72.3

Based on the ROSAT HRI observation, Hughes & Smith (1994) attributed the unresolved X-ray emission feature at $\alpha_{2000}, \delta_{2000} = 01^{\text{h}} 06^{\text{m}} 18^{\text{s}}, -72^{\circ} 06' 00''$ to emission associated with a candidate Be

star, interpreting it as a Be/X-ray star. The arcsecond resolution and good photon statistics of our deep Chandra data reveal that this X-ray emission feature is extended (Figure 1), and no point-like source is found within a few arcsecond from the position of the Be star candidate (on-axis astrometric uncertainties of the ACIS is $\sim 0.6''$). We examined the RGB composite image and various narrow band images of different energy ranges and their ratio images, but could not find any point-like feature that is positionally associated with the Be candidate. The overall X-ray spectrum of this region is also similar to X-ray spectra in other regions. Thus we conclude that the X-ray emission in this region originates from the shocked SNR gas, and not from the point source. Although the Be star that Hughes & Smith (1994) identified is unlikely to be a significant X-ray emitter, the possibility that SNR 0104-72.3 and the Be star belong to the same OB association, as they also suggested, remains valid, but would then argue against a typical Type Ia remnant. This will be further discussed in § 5.2.

The overabundance of Fe in the bar region suggests that SNR 0104-72.3 is likely the remnant of Type Ia SN. Indeed, the spectra of the bar regions are quite similar to ejecta spectra found in the well-known Type Ia SNR DEM L71 (Hughes et al. 2003) in the Large Magellanic Cloud (LMC) and several other relatively old Type Ia LMC SNRs (e.g., Borkowski et al. 2006, and references therein). DEM L71's central X-ray emission, which is well described by shocked Fe-rich ejecta, is similar to that of SNR 0104-72.3. DEM L71 also shows faint soft emission of normal LMC abundances surrounding the central emission, similar to the arc in SNR 0104-72.3. Therefore, based on the overabundant Fe from our spectral fit and the spectral similarity of the bar and the arc region to other Type Ia SNRs, we propose that SNR 0104-72.3 is the first solid candidate for Type Ia SNR in the SMC.

TABLE 1
FIT RESULTS

Region	$N_{\text{H,SMC}}$ [10^{21} cm^{-2}]	kT [keV]	Ne	Fe	$\log \tau$	norm [10^{-4}]	reduced χ^2
Arc	$9.9^{+0.22}_{-2.9}$	$0.54^{+0.05}_{-0.05}$	0.20	0.13	> 12.5	$1.4^{+0.3}_{-0.7}$	267/243
Bar	$9.1^{+1.1}_{-1.7}$	$1.95^{+0.15}_{-0.09}$	< 0.04	$1.26^{+0.11}_{-0.15}$	$11.0^{+0.1}_{-0.1}$	$0.85^{+0.05}_{-0.09}$	275/241
Bar01	9.1	$2.04^{+0.41}_{-0.24}$	0.20	$1.65^{+0.64}_{-0.35}$	$11.1^{+0.1}_{-0.1}$	$0.14^{+0.03}_{-0.04}$	280/243
Bar02	9.1	$0.72^{+0.04}_{-0.03}$	0.20	$0.51^{+0.20}_{-0.13}$	> 12	$0.36^{+0.09}_{-0.08}$	206/243
Bar03	9.1	$1.41^{+0.25}_{-0.29}$	0.20	$3.4^{+3.0}_{-0.8}$	$11.1^{+0.2}_{-0.1}$	$0.07^{+0.03}_{-0.03}$	199/243
Bar04	9.1	$1.78^{+2.30}_{-0.60}$	0.20	$0.68^{+0.34}_{-0.19}$	$11.2^{+0.1}_{-0.1}$	$0.09^{+0.17}_{-0.03}$	213/243

NOTE. — The errors are shown in 90% confidence range. Unless indicated with uncertainty values derived from the fits, the metal abundances are fixed at those of the SMC values from Russell & Dopita (1992). They are He = 0.05, C = 0.13, N = 0.20, O = 0.10, Ne = 0.20, Mg = 0.12, Si = 0.18, S = 0.15, Ar = 0.08, Ca = 0.20, Fe = 0.13, Ni = 0.20. All values are relative to the solar ones. The $N_{\text{H,SMC}}$ values for the individual bar regions (Bar01, Bar02, etc) are fixed at the value obtained for the entire bar.

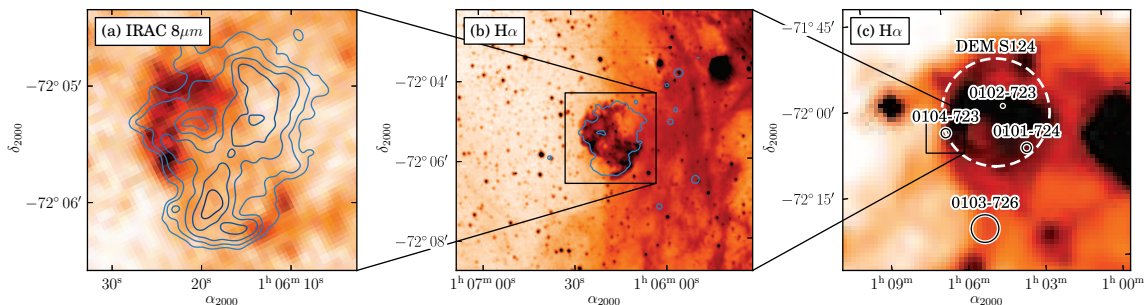


FIG. 3.— (a) Infrared image of SNR 0104-72.3 (IRAC $8\mu\text{m}$ of Spitzer archival data) with the contours of Chandra broadband image in Figure 1(a). (b) $\text{H}\alpha$ image from Hughes & Smith (1994). The lowest level contour line from (a) is shown. (c) $\text{H}\alpha$ image around SNR 0104-72.3 from the Southern $\text{H}\alpha$ Sky Survey Atlas (Gaustad et al. 2001). The solid circles are locations of known SNRs. The dashed circle is the approximate extent of the superbubble DEM S124.

Another element expected to be a signature of Type Ia SNR is Si (e.g., Badenes et al. 2007). Allowing the Si abundance to vary in the fit yields a slightly larger value, but still comparable to the SMC abundance within the fit uncertainty. The Type Ia origin is supported by non-detection of a pulsar and/or pulsar wind nebula, although they could be too faint to be detected as in other core-collapse SNRs in the SMC (e.g., Park et al. 2003).

5.2. Type Ia SNR in Unusual Environment?

Our deep Chandra observations find that the X-ray emission from the bar region is prominently from Fe-enriched SN ejecta of a Type Ia SNR. Based on limited sample, the X-ray morphologies of young Type Ia SNRs have been claimed to be statistically more symmetric than core-collapse SNRs (Lopez et al. 2009). Although a quantitative analysis of the asymmetry in the morphology of SNR 0104-72.3 should be performed (which is beyond the scope of this work), the highly elongated morphology of SNR 0104-72.3 appears to be inconsistent with the results by Lopez et al. (2009). Such an elongated Fe-rich ejecta feature is similar to that found in the Galactic SNR W49B. Although the type is uncertain for W49B (e.g., Miceli et al. 2006), the highly elongated morphology of ejecta may suggest an asymmetric explosion. Alternatively, given the possibility that the remnant is interacting with dense material toward the east (see below), the atypical morphology could be due to highly inhomogeneous ambient environment of the rem-

nant.

The environment around SNR 0104-72.3 is also unusual for a Type Ia SNR. The relatively high absorbing column density toward SNR 0104-72.3 indicates that the remnant could be located at dense environment. The eastern X-ray arc is positionally coincident with an optical and infrared shell (Figure 3). The optical emission shows dominant $\text{H}\alpha$ line with weak lines of other ions such as [O III] and [S II], and Payne et al. (2007) found that their line ratios are consistent with radiative shocks in other SNRs. Koo et al. (2007) reported infrared emission associated with SNR 0104-72.3 from their *Akari* observations. The observed infrared colors were consistent with those from shocked molecular clouds, and Koo et al. (2007) suggested that SNR 0104-72.3 is probably interacting with molecular clouds. In this regard, the radio continuum emission of SNR 0104-72.3 could be mostly from the shocked ambient gas. Although the radio data quality is poor, Figure 1(b) shows that the extent of the radio continuum covers the eastern arc region, and also the central region of the bar where the Fe overabundance appears to be less prominent. Thus, observations seem to provide a consistent picture that the arc is where the remnant is interacting with dense ambient (possibly molecular) clouds. On the other hand, the NW and SE parts of the SNR, where only the X-ray emitting ejecta are visible and there is no optical or IR emission, probably corresponds to low density regions where the forward shock in the ISM is still relatively fast and radiative shocks have

not formed.

In fact, the projected location of SNR 0104-72.3 is at the eastern boundary of the superbubble DEM S124 (Davies et al. 1976) (see Figure 3). In Figure 3(c), we show the H α emission complex toward the direction of SNR 0104-72.3 and overlay locations of known SNRs in the SMC. It appears that SNR 0104-72.3 and SNR 0102-7219, a well-known core-collapse SNR, belong to the same star-forming region. The Type Ia origin inferred from the Fe-rich ejecta and the association of the remnant with the star-forming region are not consistent with conventional scenarios of standard Type Ia, which involve the explosion of an old C/O white dwarf in a binary. Recent studies of a large sample of Type Ia SNe suggested that progenitors of some Type Ia SNe (“prompt” type) could have been relatively young massive stars

with high metallicity (e.g., Scannapieco & Bildsten 2005; Aubourg et al. 2008). More recently, from the systematic study of the SNRs in the Magellanic Clouds, Maoz & Badenes (2010) suggested that some of the SNRs could be remnants of the prompt Type Ia SNe. While we cannot completely rule out the possibility of mere coincidence, the unusual nature of SNR 0104-72.3 (i.e., Type Ia characteristics of Fe-rich X-ray ejecta in the SNR and the SNR’s spatial association with an environment with a strong star-forming activity) suggests an intriguing possibility that SNR 0104-72.3 may be a candidate SNR of a prompt SN Ia.

This work was supported in part by the Smithsonian Astrophysical Observatory under Chandra grant GO8-9509A. P.O.S. acknowledges partial support from NASA contract NAS8-03060.

REFERENCES

- Aubourg, É., Tojeiro, R., Jimenez, R., Heavens, A., Strauss, M. A., & Spergel, D. N. 2008, *A&A*, 492, 631
- Badenes, C., Borkowski, K. J., Hughes, J. P., Hwang, U., & Bravo, E. 2006, *ApJ*, 645, 1373
- Badenes, C., Hughes, J. P., Bravo, E., & Langer, N. 2007, *ApJ*, 662, 472
- Bock, D., Large, M. I., & Sadler, E. M. 1999, *AJ*, 117, 1578
- Borkowski, K. J., Hendrick, S. P., & Reynolds, S. P. 2006, *ApJ*, 652, 1259
- Borkowski, K. J., Lyerly, W. J., & Reynolds, S. P. 2001, *ApJ*, 548, 820
- Churazov, E., Gilfanov, M., Forman, W., & Jones, C. 1996, *ApJ*, 471, 673
- Davies, R. D., Elliott, K. H., & Meaburn, J. 1976, *MmRAS*, 81, 89
- Dickey, J. M., & Lockman, F. J. 1990, *ARA&A*, 28, 215
- Gaustad, J. E., McCullough, P. R., Rosing, W., & Van Buren, D. 2001, *PASP*, 113, 1326
- Hughes, J. P., Ghavamian, P., Rakowski, C. E., & Slane, P. O. 2003, *ApJ*, 582, L95
- Hughes, J. P., & Smith, R. C. 1994, *AJ*, 107, 1363
- Koo, B., Lee, H., Moon, D., Lee, J., Seok, J. Y., Lee, H. M., Hong, S. S., Lee, M. G., Kaneda, H., Ita, Y., Jeong, W., Onaka, T., Sakon, I., Nakagawa, T., & Murakami, H. 2007, *PASJ*, 59, 455
- Lopez, L. A., Ramirez-Ruiz, E., Badenes, C., Huppenkothen, D., Jeltema, T. E., & Pooley, D. A. 2009, *ApJ*, 706, L106
- Maoz, D., & Badenes, C. 2010, *MNRAS*, 407, 1314
- Mathewson, D. S., Ford, V. L., Dopita, M. A., Tuohy, I. R., Mills, B. Y., & Turtle, A. J. 1984, *ApJS*, 55, 189
- Miceli, M., Decourchelle, A., Ballet, J., Bocchino, F., Hughes, J. P., Hwang, U., & Petre, R. 2006, *A&A*, 453, 567
- Park, S., Hughes, J. P., Burrows, D. N., Slane, P. O., Nousek, J. A., & Garmire, G. P. 2003, *ApJ*, 598, L95
- Payne, J. L., White, G. L., Filipović, M. D., & Pannuti, T. G. 2007, *MNRAS*, 376, 1793
- Russell, S. C., & Dopita, M. A. 1992, *ApJ*, 384, 508
- Scannapieco, E., & Bildsten, L. 2005, *ApJ*, 629, L85
- Smith, R. K., Brickhouse, N. S., Liedahl, D. A., & Raymond, J. C. 2001, *ApJ*, 556, L91
- Stanimirovic, S., Staveley-Smith, L., Dickey, J. M., Sault, R. J., & Snowden, S. L. 1999, *MNRAS*, 302, 417
- van der Heyden, K. J., Bleeker, J. A. M., & Kaastra, J. S. 2004, *A&A*, 421, 1031